Mon. Not. R. Astron. Soc. **000**, 000–000 (0000) Printed 15 August 2013 (MN LATEX style file v2.2)

The Fundamental Manifold of spiral galaxies: ordered versus random motions and the morphology dependence of the Tully-Fisher relation.

C. Tonini[1] ⋆, D. H. Jones[2], J. Mould[1], R. L. Webster[3], T. Danilovich[4], and S. Ozbilgen[3]

[1] *Centre for Astrophysics and Supercomputing, Swinburne University of Technology, Hawthorn, VIC 3122, Australia*
[2] *School of Physics, Monash University, Clayton, VIC 3800, Australia*
[3] *School of Physics, University of Melbourne, Parkville, 3010 VIC, Australia*
[4] *Chalmers University, Maskingrand 2, 412 58 Goteborg, Sweden*

15 August 2013

ABSTRACT

We investigate the morphology dependence of the Tully-Fisher (TF) relation, and the expansion of the relation into a three-dimensional manifold defined by luminosity, total circular velocity and a third dynamical parameter, to fully characterise spiral galaxies across all morphological types. We use a full semi-analytic hierarchical model (based on Croton et al. 2006), built on cosmological simulations of structure formation, to model galaxy evolution and build the theoretical Tully-Fisher relation. With this tool, we analyse a unique dataset of galaxies for which we cross-match luminosity with total circular velocity and central velocity dispersion. We provide a theoretical framework to calculate such measurable quantities from hierarchical semi-analytic models. We establish the morphology dependence of the TF relation in both model and data. We analyse the dynamical properties of the model galaxies and determine that the parameter $\sigma/V_{\rm C}$, i.e. the ratio between random and total motions defined by velocity dispersion and circular velocity, accurately characterises the varying slope of the TF relation for different galaxy types. We apply these dynamical cuts to the observed galaxies and find indeed that such selection produces a differential slope of the TF relation. We conclude that the $\sigma/V_{\rm C}$ is a suitable parameter to characterise the hierarchical assembly history that determines the disk-to-bulge ratio, and to to expand the TF relation into a three-dimensional manifold, defined luminosity, circular velocity and $\sigma/V_{\rm C}$. We also conclude that $\sigma/V_{\rm C}$ is a good parameter to classify galaxy morphology, and it produces consistent results with the traditional Sa, Sb, Sc classification. We argue that this method of classification is useful for galaxy evolution and TF studies at higher redshifts, where eye inspection of the data to determine galaxy morphology is not reliable, and for large survey datasets, where it is impractical.

Key words: galaxies: formation galaxies: evolution galaxies: kinematics and dynamics galaxies: structure galaxies: fundamental parameters galaxies: photometry

1 INTRODUCTION

Galaxy scaling relations highlight the regularities that characterise galaxy formation. Of particular interest is the physical connection between the dynamical state of a galaxy, determined by its assembly history, and the galaxy photometric properties, tracing its stellar populations and its star formation history. The main dynamical quantity in such an analysis is the galaxy total gravitational potential, which determines the galaxy rotation curve. In the case of spiral galaxies, this is usually parameterised with the circular velocity at a given radius, and in the case of ellipticals, with the central velocity dispersion. Both these quantities have a monothonic dependence on luminosity, thus giving rise to the Tully-Fisher relation (TF; Tully & Fisher, 1977) for spi-

⋆ E-mail:ctonini@astro.swin.edu.au

rals, and the Faber-Jackson relation (FJ; Faber & Jackson 1976) for ellipticals.

However galaxy structure cannot be completely captured by such simple scalings, and the underlying complexity emerges with additional parameters. In the case of ellipticals, the triaxial mass distribution causes an expansion of the FJ relation into a third dimension, recasting it as a scaling between velocity dispersion σ, surface brightness I_e and effective radius r_e, known as the Fundamental Plane (FP; Djorgovski & Davis 1987, Dressler et al. 1987), a manifestation of the virial theorem in observational quantities (see for instance Cappellari et al. 2006). The slope of the FP indicates that the structure of elliptical galaxies is not a self-similar scaled version of a single object as a function of mass.

In the case of spirals, the apparent simplicity of these systems is broken by the observational evidence of a morphology dependence of the TF slope (Springob et al. 2007, Masters et al. 2008). Such feature is also predicted by hierarchical galaxy formation models (Tonini et al. 2011), which naturally produce a varying TF slope that depends on the galaxy internal dynamics, a signature of its assembly history. Indeed, there is an extensive body of work in the literature supporting the observational evidence of a dependence of the TF on galaxy type; the TF for late-type spirals (Masters et al. 2006, Courteau 1997, Giovanelli et al. 1997) is not followed by early-type spirals and S0 types (Williams et al. 2010, Bedregal et al. 2006, Neistein et al. 1999), dwarf galaxies (McGaugh et al. 2000, Begum et al. 2008), barred spirals (Courteau et al. 2003), and polar ring galaxies (Iodice et al. 2003).

The evidence suggests that a third parameter beside circular velocity and luminosity enters the TF relation. This parameter depends on galaxy type, and expands the TF into a three-dimensional manifold that describes the structure of spirals or alternatively, of all galaxies. A general three-dimensional manifold for galaxies regardless of type has been investigated (see Zaritsky et al. 2008), with the set of observables (V_c, I_e, r_e) in analogy with the ellipticals FP. The approach of this work is the use of analytic toy models, which cannot capture the intrinsic complexity of galaxies due to their hierarchical mass assembly, but resort to absorb it into a single parameter, Γ_e, the mass-to-light ratio inside the half-light radius r_e, and to fit this parameter assuming that galaxies lie on the manifold. Catinella et al. (2012) make use instead of dynamical indicators such as rotational velocity and dispersion to obtain a generalised baryonic FJ relation that holds for all galaxy types. Courteau et al. (2007) investigate galaxy size, and analyse the spiral size-luminosity and luminosity-velocity relations and their dependence on morphology and stellar population content.

In this work we consider two questions: 1) is there a third dynamical parameter that characterises the morphology-dependence of the Tully-Fisher relation, and can be used to expand such relation into a three-dimensional manifold, describing the structure of spiral galaxies?; and 2) can we use this parameter to classify galaxy morphology, when visualisation is not available (for instance at high redshift) or impractical (for instance for large surveys)?

The novelty of our analysis is that we take advantage of a full semi-analytic hierarchical model (based from Croton et al. 2006) to define a dynamical parameter that characterises galaxy morphology, predicts the TF relation for different galaxy types and defines the spiral galaxy manifold. The model is built on cosmological simulations of structure formation, to model galaxy formation and evolution and build the theoretical TF relation. This tool is ideal for accounting for the merger history of galaxies and their complex star formation history, which is recorded in their rotation curve and stellar populations. We take particular care in producing dynamical and photometric quantities that can be directly compared with observations. With this tool, we analyse a unique dataset of galaxies: we build a sample of observed galaxies carrying the information on luminosity, circular velocity and central velocity dispersion, derived from the GALEX Arecibo SDSS Survey (Catinella et al. 2013). To this sample we apply our theoretical predictions.

In Section 2 we describe the model. In Section 3 we introduce our observational sample and present our main results. In Section 4 we discuss our findings and present our conclusions.

2 THE MODEL

Semi-analytic models are a powerful tool for investigating the TF relation in a cosmological framework. They naturally interlink the dynamics of structure formation with the galaxy emission; the galaxy assembly and star formation histories derive directly from the hierarchical growth of structures. In addition, such models allow for a thorough statistical analysis. The model galaxies are obtained with the semi-analytic model by Croton et al. (2006), with the spectro-photometric model (including dust absorption and emission) described in Tonini et al. (2012). We implement the prescription for the galaxy rotation curves by Tonini et al. (2011), where the velocity profile is determined by the mass distribution of all galaxy components (dark matter, stellar disk and bulge, and gas), and the total circular velocity is

$$V_C^2(r) = V_{\rm DM}^2(r) + V_{\rm disk}^2(r) + V_{\rm bulge}^2(r) \quad (1)$$

(see also Tonini et al. 2006a, Salucci et al. 2007). The slope of the TF relation, and in particular its tilting with galaxy type observed in the data, is the manifestation of the connection between galaxy dynamics and star formation and assembly history. For spiral galaxies in general, morphology can be understood in terms of bulge-to-disk ratios. Dynamically, the growth of a bulge in the center of a disk is the result of secular (angular momentum redistribution and stellar migration, bars) and violent (mergers) processes, all of which leave a trace in the galaxy rotation curve. At the same time, the star formation history of the galaxy, which is affected by the dynamical evolution, imprints the bulge-to-disk luminosity. A theoretical determination of the TF relation needs to incorporate each of these effects to be successful, a job that hierarchical semi-analytic models are best suited to accomplish.

2.1 Which radius? An angular momentum problem

When studying the morphology dependence of the TF relation, it becomes especially important to measure the TF at

a meaningful, physically motivated radius. Because of the different radial profiles of the galaxy dynamical components (disk, bulge, dark matter halo, gas), *1)* the slope of the TF relation varies with the radius at which the rotation velocity is calculated (Yegorova et al. 2007) and *2)* the same radius in galaxies of different morphology probes different dynamical regions, thus introducing an artificial scatter in the TF. Traditionally, the velocity at a galactocentric radius $r = 2.2R_{\rm D}$, where $R_{\rm D}$ is the exponential stellar disk scale-length, has often been used to build the TF relation from observations. This velocity roughly corresponds to the peak velocity of a bulgeless disk; in the case of a galaxy with a substantial bulge however, the region around $r = 2.2R_{\rm D}$ contains a different mix of dark matter, gas and stars, and the peak of the rotation curve is actually at a different radius.

Following Tonini et al. (2011), we adopt a *dynamical* definition of the disk scale-length, that corresponds to a *fixed angular momentum* rather than a fixed galactocentric distance. With this definition the value of $R_{\rm D}$ self-regulates in the presence of a bulge. The formation of the bulge, both from secular evolution and mergers, implies that stars migrate radially or with inspiralling orbits to the centre of the galaxy, losing all their angular momentum and settling into a pressure-supported configuration. This lost angular momentum is transferred to the disk (Dutton et al. 2007; see also Tonini et al. 2006), with the net effect of increasing the disk size. For a bulge of mass $M_{\rm bulge}$ forming in a disk of mass $M_{\rm disk}$ with initial scale-length $R_{\rm D_{old}}$, the disk scale-length after angular momentum transfer is

$$R_{\rm D} = R_{\rm D_{old}} \left(1 + (1 - f_{\rm x})\frac{M_{\rm bulge}}{M_{\rm disk}}\right) , \qquad (2)$$

with the fiducial value $f_{\rm x} = 0.25$ indicated by Dutton et al. (2007). The new $R_{\rm D}$ represents a 'corrected' disk scale-length, that takes into account the additional gravitational potential of the bulge. After the correction, all galaxies move onto the disk mass-disk scale length relation that holds for Sc galaxies (see Tonini et al. 2011). After defininining a $R_{\rm D}$ that evolves with morphology, it then makes physical sense to adopt $r = 2.2R_{\rm D}$ as our radius of choice to build the TF relation.

2.2 Integrated galaxy velocity dispersion

From the mass distribution we can build velocity profiles for all galaxy components. The theoretical velocity dispersion is the sum of the contribution to the rotation curve by all components that are pressure-supported, namely the dark matter halo and the bulge:

$$\sigma(r) = \sqrt{V^2_{\rm DM}(r) + V^2_{\rm bulge}(r)} , \qquad (3)$$

where each velocity term in the equation is determined by the mass profile of the dynamical component: $V_i^2(r) \propto GM_i(r)/r$ (see Tonini et al. 2011 for a detailed description). However this particular kind of output is not readily comparable with observations. In fact, in the literature the observed samples usually provide a single-value galaxy velocity dispersion for each object, which is obtained from the broadening of distinct spectral features due to the internal motions of the stars. This measure is an integrated quantity over a galactocentric radius generally determined by telescope aperture or detection limit. The model on the other hand outputs intrinsic, physical galaxy properties, thus the comparison with the observed spectral line dispersion requires *1)* the definition of a 'model aperture radius' inside which to compute the velocity dispersion, and *2)* the definition of an integrated velocity dispersion inside this radius.

In defining such a radius, there are two factors to consider: *1)* the galaxy dynamics becomes increasingly dark matter-dominated at larger galactocentric distances, but *2)* the only visible tracers of the galaxy velocity dispersion are the stars in the bulge, since the disk is modeled as completely rotation-supported. Therefore, if we were to 'observe' a model galaxy, the entirety of the velocity dispersion signal in the spectral features would come from the stars in the bulge. For this reason, we assume that the 'model aperture radius' corresponds to the bulge outer limit, which we define as $3.5{\rm R_{bulge}}$. Note that this definition implies a different radius for each galaxy, and simply corresponds to the assumption that the aperture is always larger than the target. In observations on the contrary the aperture radius is fixed, and this factor contributes to the observed scatter in the Tully-Fisher.

The width of a spectral line is in principle obtained by averaging the velocity dispersion over all the stars; however in models, that calculate theoretical velocity dispersion profiles, the definition is not as straightforward. We opt for calculating the mass-averaged velocity dispersion over radial bins out to the bulge outer limit:

$$\sigma = \frac{\sum_n M_n\ \sigma_n}{\sum_n M_n} , \qquad (4)$$

where M_n is the total mass in the *nth* shell (out to the bulge outer limit), and σ_n is the total velocity dispersion in the centre of the bin, as calculated from the bulge and halo velocity profiles (see Tonini et al. 2011). This definition ensures that σ is naturally dominated by the sections of the density profile that contribute the most to the velocity dispersion profile. Note also that a quantity more directly comparable with data would be a luminosity-averaged dispersion, but this would require an additional layer of modeling (in particular a modeling of the radial dependence of the mass-to-light ratio), that is not very well constrained and represents an important source of scatter.

2.3 Selection of the model galaxies

In the model, morphology can be defined in terms of the galaxy physical parameters, like the mass of the bulge and the disk (see Tonini et al. 2011). This method has the advantage of grouping together objects that share a similar formation history, thus favouring a more detailed study of the physics involved in their evolution. On the other hand, this type of selection is hard to apply to observations, and it involves some model-dependencies in the conversion between colors and luminosities to masses and ages, thus confusing the comparison between models and data.

In most observations the determination of the Hubble type employs the use of some photometric criterion, based on colors or on the relative luminosities of bulge and disk when available. To facilitate the comparison, we classify our model galaxies with one of such methods, based on the bulge-to-total luminosity ratio in the B band, following Simien & De Vaucouleurs (1986): after defining $\mu_B =$

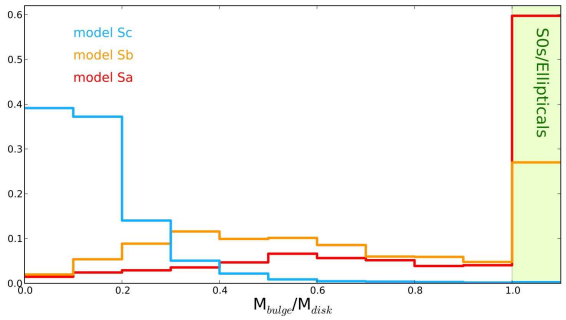

Figure 1. The distribution of the mass ratio $M_{\rm bulge}/M_{\rm disk}$ for the model Sc, Sb and Sa galaxies (*blue, orange and red respectively*).

$M_B(bulge) - M_B(total)$, Sc galaxies are characterised by $2.3 < \mu_B < 4.15$, Sb galaxies by $1.23 < \mu_B < 2.01$ and Sa galaxies by $0.8 < \mu_B < 1.23$. In Fig. (1) we compare this classification with the actual mass ratio of bulge and disk, M_{bulge}/M_{disk}. We find that the Sc type is well represented by galaxies with small bulges (less than $\sim 20\%$ of the disk mass). On the other hand, Sb types show a wide variety of bulge-to-disk ratios (peaking between 0.2 and 0.7), and Sa galaxies are rare below 1, where they show a very flat distribution. Both Sb and Sa types leak into the S0 and elliptical regimes, defined in the model for values $M_{bulge}/M_{disk} > 1$. It is not difficult to imagine that such a scenario is present in observed galaxies too, expecially if the photometric band used for the selection evolves rapidly and is subject to dust extinction, like the B band. The photometric definition of Sb and Sa model galaxies select objects that do not belong to a uniform population in terms of physical parameters and formation history. We believe this is the origin of the increased observed scatter in the TF relation for these galaxy types.

3 RESULTS

To compare the model with observed data, we employ the sample of GASS (GALEX Arecibo SDSS) survey, Data Release 3 (Catinella et al. (2013; see also Catinella et al. 2010 for a complete description of the survey), which provides circular velocities obtained from HI linewidths. To this sample we add measurements of the central velocity dispersions measurements from the Sloan Digital Sky Survey, Data Release 9 (Ahn et al. 2012), and K-band magnitudes from the Two Micron All Sky Survey (2MASS; Skrutskie et al. 2006). Distances are estimated from the 21 cm redshifts (see Mould et al 2000). To minimise the scatter we consider only galaxies with inclinations $> 45°$. The final sample after cutting away non-detections and poor-quality detections (see Catinella et al. 2013) consists of ~ 340 galaxies.

Note that this is not a Tully-Fisher dedicated sample, and galaxies were not selected based on the quality of their rotation curves or their morphological type. The goal in this work is to characterise the physical properties of the galaxies in this sample so that they would naturally produce a morphology-dependent TF relation. In other words, we want to find the physical parameters that uniquely characterise the Tully-Fisher manifold of spiral galaxies, by which Sa, Sb and Sc samples can be extracted from any dataset without the aid of visual inspection. How can we characterise a galaxy (type, morphology, history) for instance at high redshift, or for large datasets when visualisation becomes impractical?

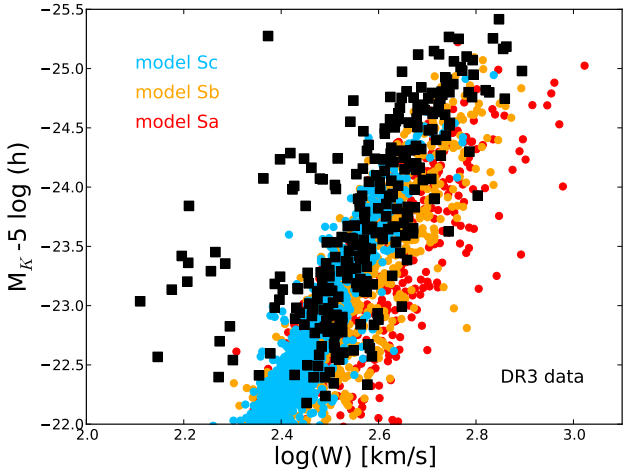

Figure 2. The Tully-Fisher relation for the semi-analytic model galaxies, divided according to morphology (*light blue, orange and red points* for Sc, Sb and Sa galaxies respectively), compared with the observed sample (*black squares*).

We start by building the TF relation for the observed sample, plotted in Fig. (2) in terms of $W = 2V_{\rm C}$ and represented by the *black squares*. Note that the majority of the galaxies in the sample follow a reasonably-defined relation, but with a rather large scatter. In addition, there are numerous objects that significantly deviate from such behaviour. Fig. (2) also shows the Tully-Fisher relation for the model galaxies, divided according to morphology: *light blue, orange and red points* represent Sc, Sb and Sa galaxies respectively. The presence of larger bulges tends to flatten the slope of the TF relation, by increasing the mass-to-light ratio, and at the same time is a source of scatter both in luminosity and circular velocity. Model and data roughly occupy the same locus in the plot (ignoring the data outliers for the moment), so we use the model to provide insight into the observed galaxies.

In the model, the galaxy type and its evolutionary history (short *vs* prolongued star formation history, merger-rich *vs* merger-poor assembly) is at first order characterised by the mass ratio between the spherical and disky components $M_{\rm bukge}/M_{\rm disk}$. A more observationally-friendly quantity to express this is the ratio between random and total motions. In the model this corresponds to $\sigma/V_{\rm C}$, where σ is defined by Eq. (3), and $V_{\rm C}^2 = \sigma^2 + V_{\rm disk}^2$ (Eq. (1)). The bulge and dark matter halo mostly contribute with velocity dispersion, and the disk mostly with rotation.

After splitting the model galaxies in photometric classes Sa, Sb and Sc, we consider the ratio $\sigma/V_{\rm C}$ for each type, and plot it in Fig. (3), as a function of the total circular velocity $V_{\rm C}$, calculated at 2.2 $R_{\rm D}$ (where $R_{\rm D}$ is defined by Eq. (2)); these are the *open circles, colour-coded as in Fig. (2)*. The model galaxies show a differentiation in $\sigma/V_{\rm C}$ depending on the B-band selected morphology, with later-type spirals

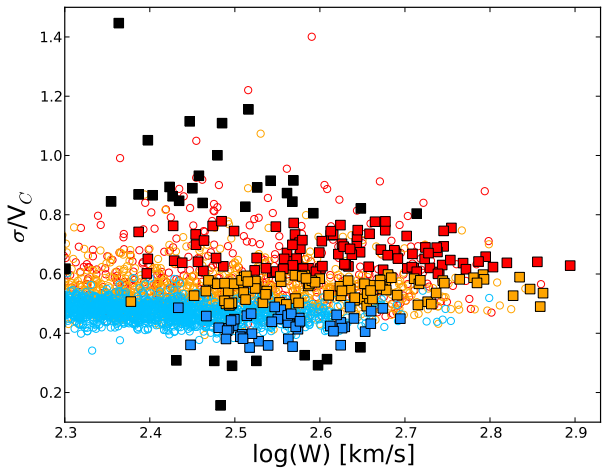

Figure 3. The ratio of velocity dispersion and circular velocity as a function of $W = 2V_{\rm C}$, for the model galaxies (*open circles, colour-coded as in Fig. (2)*) and for the observed sample (*squares, colour coded depending on the locus they share with the model*). Data outliers are represented in *green*.

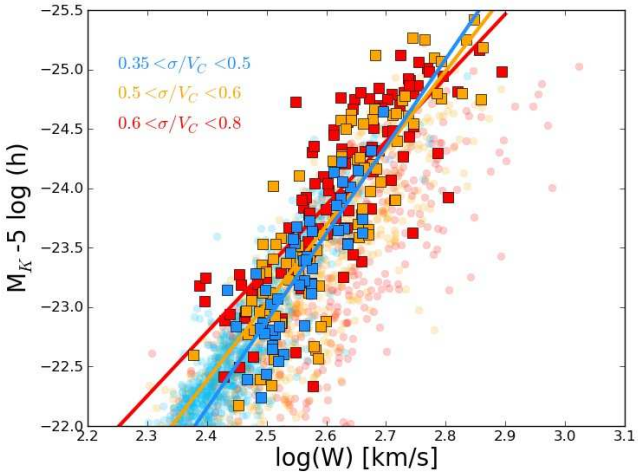

Figure 4. The TF relation for the observed sample, after splitting it into morphological types based on the model $\sigma/V_{\rm C}$, as in Fig. (3). The lines represent linear regression fits. The colour-coding is the same as in Fig. (3).

showing a smaller total velocity dispersion than the earlier types, for a given total circular velocity, and a smaller scatter. This shows how dynamics and star formation history are interlinked in the model: the hierarchical build-up of galaxies grows bulges and evolves the star formation rates to produce redder early-type objects. Moreover, following the nature of hierarchical mass assembly, bigger bulges are accompanied by larger scatter in the $\sigma/V_{\rm C}$. Notice, however, how there is no clear mass-dependence of $\sigma/V_{\rm C}$ for a given morphological type.

We then compare the observed sample in the same space (*squares*), and we colour-code the data based on where they lay with respect to the model, in bands of $\sigma/V_{\rm C}$. We colour in *green* the outliers, i.e. galaxies that do not fall in the locus of the model (those with $\sigma/V_{\rm C} > 0.8$ and $\sigma/V_{\rm C} < 0.35$), and a handful which a visual inspection reveals to be perturbed or missclassified in terms of inclination. We also consider as outliers all objects with $V_{\rm C} < 100\ km/s$, which fall way off both the bulk of the data and the model in the TF plot (Fig. (2); moreover, the model starts to suffer from resolution effects at those masses, given the mass resolution of the Millennium simulation).

The outliers are mostly dispersion-dominated (in accord with the analysis by Catinella et al. 2012), a feature that in the model is a signature of an early-type/elliptical galaxy. A few outliers show instead a very low velocity dispersion. However, in the range of circular velocities considered here, ratios $\sigma/V_{\rm C} < 0.35$ yield velocity dispersions $\sigma < 70\ km/s$, which is the resolution limit of the Sloan spectrograph. For this reason, such values of the velocity dispersion cannot be considered reliable (Bernardi et al. 2003).

or have a negligible amount of velocity dispersion compared to the total circular velocity. The latter might be a signature of a bulgeless galaxy, for which the total dispersion cannot be traced with the bulge stars as accurately as for earlier types. However, this might also be a

Is $\sigma/V_{\rm C}$ a good parameter to characterise observed galaxies? In other words, have we selected a spiral sample, based entirely on theoretical expectations of the ratio between random and total motions? And is this classification a good proxy for galaxy morphology, i.e. will the sub-classes produce different TF relations?

Fig. (4) shows again the TF relation for the observed sample, after we have divided the galaxies in bands of $\sigma/V_{\rm C}$, following the prediction of the semi-analytic model described in Fig. (3).

Indeed, the three subsamples follow three distinct TF relations. As bulges grow larger in galaxies, the TF slope flattens as expected, mostly due to the increased mass-to-light ratio due to the spherical component. At the same time, the scatter increases due to the hierarchical nature of galaxy assembly, more prominent in bulge-heavy galaxies because the bulge is a signature of a significant merger history (Tonini et al. 2011; see also Tonini, 2013).

A linear regression of the TF relation for the three subsamples yields the values [-5.35 ± 0.40, -6.50 ± 0.42, -7.34 ± 0.72] for the TF slope of Sa, Sb and Sc-types respectively (also consistent with the theoretical values obtained in Tonini et al. 2011, and the observations of Masters et al. 2008). The best fit lines are shown in the plots in *red, orange and light blue* respectively. The model galaxies are shown in the background, colour-coded as usual.

The slopes and zero-points for the more rotationally-supported objects (*light blue and orange lines*) are well matched with the model Sc and Sb TF relations. The TF slope for the observed more dispersion-dominated objects is shallower and consistent with that of model Sa galaxies, although the zero-point is offset by about 0.5 *mag* or by 50% in the velocity. This might be due to selection effects. In fact, the GASS sample was selected based on the HI signature; while in the model Sc and Sb galaxies are pretty uniformly gas-rich, the earlier types present a larger scatter in gas content, depending on the assembly history, and therefore this class of model objects cannot be matched in its entirety by the GASS sample.

Fig. (4) shows that $\sigma/V_{\rm C}$ is a good dynamical parameter to characterise spiral galaxies, and it is a good proxy for morphology. The data selected based on $\sigma/V_{\rm C}$ produces morpholgy-dependent TF relations, consistent with the theoretical expectations and previous observational results. The spiral galaxy scaling relation between luminosity and dynamics seems fully characterised in the three-dimensional space $[M_{\rm K}, V_{\rm C}, \sigma/V_{\rm C}]$ across all spiral types.

4 DISCUSSION AND CONCLUSIONS

The Tully-Fisher relation is the product of virial equilibrium combined with the star formation history. It links a measure of the total gravitational potential, $V_{\rm C}$, with the stellar mass as a function of age, expressed by the luminosity in various bands. The fact that the TF relation holds for all spirals shows that there is one principal parameter that largely governs galaxy evolution, i.e. the total mass. On the other hand, the perturbations in the TF, such as the observed morphology dependence, indicate that at least a second parameter plays a detectable role. Such parameter is linked to the mass *distribution* inside the galaxy, a product of both secular evolution and hierarchical mass assembly (an ideal scenario to study with a semi-analytic model).

The mass distribution might be parameterised with some definition of effective radius, as in the case or ellipticals, but this method relies on a photometric classification that in both models and observations is affected by systematics. Another route is to consider that mass distribution is interlinked with the distribution of the internal motions. In these terms, a dynamical parameter such as $\sigma/V_{\rm C}$ represents as well the mass concentration as the fraction of random over total motions inside the galaxy. In the formalism of virial equilibrium phase-space analysis, it represents an angular momentum parameter. This makes it a very clear-cut, physically well defined quantity to determine in models, but it also has observational advantages. In fact, while a morphology analysis or the determination of effective radii is very uncertain for distant galaxies, central velocity dispersion and circular velocity are relatively easy to determine from galaxy spectra, pushing the analysis of the TF relation to higher redshifts. In addition, this method is ideal in the case of large galaxy surveys, where a classification based on visual inspection is impractical.

The parameter $\sigma/V_{\rm C}$ tracks the emission of a fraction of the stellar populations, those that are not rotationally supported. These are mostly the bulge stars, a component of intermediate to old age, with a higher mass-to-light ratio than the disk. The prominence of this component causes the velocity-luminosity relation to shift from that of the Sc types (close to pure disks). $\sigma/V_{\rm C}$ is a good proxy for galaxy morphology, it directly relates to the bulge-to-total mass ratio, which can be linked with some degree of accuracy to the bulge-to-disk luminosity ratios traditionally used in the morphology classifications. For this reason the varying slope of the TF relation according to $\sigma/V_{\rm C}$ corresponds to that seen for different morphology types classified according to luminosity ratios.

Notice in addition that $\sigma/V_{\rm C}$ can be used to expand the present analysis to S0 and elliptical galaxies, where $M_{\rm bulge}/M_{\rm disk} > 1$. A future work will address the determination of a galaxy manifold including all galaxy types, defined by $[L, V_{\rm C}], \sigma/V_{\rm C}$, and based on a larger observed galaxy sample.

The aim of this work is to characterise the morphology dependence of the Tully-Fisher relation with a physical parameter, and employ it along with circular velocity and luminosity to define a three-dimensional manifold that determines the structure of spiral galaxies. We built and analysed a sample of observed galaxies and compared the observed Tully-Fisher relation and the central galaxy velocity dispersion with the predictions by a hierarchical semi-analytic model based on Croton et al. (2006). Our results are the following:

- the model predicted K-band TF relation is a good match to the data; the hierarchical galaxy formation model fully captures the velocity-luminosity relation for spirals. The model galaxies, classified as Sa, Sb and Sc galaxies with a photometric criterium, show a differentiation of the TF slope, zero-point and scatter with the galaxy type;
- we define a theoretical galaxy velocity dispersion as the component of the rotation curve generated by the spherical, pressure supported mass components, i.e. bulge and dark matter halo, and traced by the stars in the bulge; to compare it with the central (aperture-defined) velocity dispersion measured from galaxy spectra, we compute the mass-average of such component over its density profile;
- we compare the observed ratio of the velocity dispersion over total circular velocity $\sigma/V_{\rm C}$, as a function of $V_{\rm C}$, with the predictions of the semi-analytic model, finding a good match. The model predicts a segregation of $\sigma/V_{\rm C}$ as a function of galaxy type, with the earlier-types exhibiting a higher $\sigma/V_{\rm C}$ and a larger scatter;
- we divide the observed galaxies in 3 subsamples of different average $\sigma/V_{\rm C}$ following the model trend, and recalculate the TF relation separately for the 3 subsamples; we find that they follow 3 distinct TF relation, with decreasing slope for increasing $\sigma/V_{\rm C}$. In addition, this method naturally exclude the TF outliers, thus reducing the scatter on the TF relation;
- we find that $\sigma/V_{\rm C}$ is a good dynamical parameter characterising galaxy morphology, yielding a classification consistent with the photometrically defined Sa, Sb and Sc types.

We conclude that $\sigma/V_{\rm C}$ is a good, physically motivated third parameter to characterise the TF across the spiral galaxy population. Along with the total velocity $V_{\rm C}$ and the luminosity $M_{\rm K}$, $\sigma/V_{\rm C}$ it thus defines a three-dimensional spiral galaxy manifold that fully characterise the spiral population.

ACKNOWLEDGMENTS

We would like to thank Barbara Catinella, Simon Mutch and Darren Croton for their insight and the useful discussions. JM is funded by the Australian Research Council Discovery Projects. This publication makes use of data products from the Two Micron All Sky Survey, which is a joint project of the University of Massachusetts and the Infrared Processing and Analysis Center/California Institute of Technology, funded by the National Aeronautics and Space Administration and the National Science Foundation. This research

has made use of the NASA/ IPAC Infrared Science Archive, which is operated by the Jet Propulsion Laboratory, California Institute of Technology, under contract with the National Aeronautics and Space Administration. Funding for SDSS-III has been provided by the Alfred P. Sloan Foundation, the Participating Institutions, the National Science Foundation, and the U.S. Department of Energy Office of Science. The SDSS-III web site is http://www.sdss3.org/. SDSS-III is managed by the Astrophysical Research Consortium for the Participating Institutions of the SDSS-III Collaboration including the University of Arizona, the Brazilian Participation Group, Brookhaven National Laboratory, Carnegie Mellon University, University of Florida, the French Participation Group, the German Participation Group, Harvard University, the Instituto de Astrofisica de Canarias, the Michigan State/Notre Dame/JINA Participation Group, Johns Hopkins University, Lawrence Berkeley National Laboratory, Max Planck Institute for Astrophysics, Max Planck Institute for Extraterrestrial Physics, New Mexico State University, New York University, Ohio State University, Pennsylvania State University, University of Portsmouth, Princeton University, the Spanish Participation Group, University of Tokyo, University of Utah, Vanderbilt University, University of Virginia, University of Washington, and Yale University.

REFERENCES

Ahn, C. P., et al., 2012, ApJS, 203, 21A
Bedregal, A. G., Aragon-Salamanca, A. & Merrifield, M. R., 2006, MNRAS, 373, 1125
Begum, A., Chengalur, J. N., Karachentsev, I. D. & Sharina, M. E., 2008, MNRAS, 386, 138
Bernardi, M., et al., 2003, AJ, 125, 1817
Cappellari, M., et al., 2006, MNRAS, 366, 1126C
Catinella, B., et al., 2010, MNRAS, 403, 683
Catinella, B., et al., 2012, MNRAS, 420, 1959C
Catinella, B., et al., 2013ArXiv1308.1676C
Courteau, S., 1997, AJ, 114, 2402
Courteau, S., Andersen, D. R., Bershady, M. A., MacArthur, L. A. & Rix, H.-W., 2003, ApJ, 594, 208
Courteau, S., Dutton, A. A., van den Bosch, F. C., MacArthur, L. A., Dekel, A., McIntosh, D. H. & Dale, D. A., 2007, ApJ, 671, 203
Croton, D. J., Springel, V., White, S. D. M., De Lucia, G., Frenk, C. S., Gao, L., Jenkins, A., Kauffmann, G., Navarro, J. F. & Yoshida, N., 2006, MNRAS, 365, 11
Dressler, A., Lynden-Bell, D., Burstein, D., Davies, R. L., Faber, S. M., Terlevich, R. & Wegner, G., 1987, ApJ, 313, 42
Dutton, A.A., van den Bosch, F.C., Dekel, A. & Courteau, S., 2007, ApJ, 654, 27D
Djorgovski, S. & Davis, M., 1987, ApJ, 313, 59D
Faber, S. M. & Jackson, R. E., 1976, ApJ, 204, 668F
Giovanelli, R., Haynes, M. P., Herter, T., Vogt, N. P., da Costa, L. N., Freuding, W., Salzer, J. J. & Wegner, G., 1997, AJ, 113, 53
Iodice, E., Arnaboldi, M., Bournaud, F., Combes, F., Sparke, L. S., van Driel, W. & Capaccioli, M., 2003, ApJ, 585, 730
Maraston, C. 2005, MNRAS, 362, 799
Masters, K.L., Springbob, C. M., Haynes, M. P. & Giovanelli, R., 2006, ApJ, 653, 861
Masters, K.L., Springbob, C.M. & Huchra, J.P., 2008, AJ, 135, 1738M
McGaugh, S. S., Schombert, J. M., Bothun, G. D. & de Blok, W. J. G., 2000, ApJ, 533, L99
Mould, J. R., et al., 2000, ApJ, 529, 786M
Neistein, E., Maoz, D., Rix, H.-W. & Tonry, J. L., 1999, AJ, 117, 2666
Salucci, P., Lapi, A., Tonini, C., Gentile, G., Yegorova, I. & Klein, U., 2007, MNRAS, 378, 41S
Simien, F. & de Vaucouleurs, G., 1986, ApJ, 302, 564S
Skrutskie, M. F., et al., 2006, AJ, 131, 1163
Springob, C. M., Masters, K. L., Haynes, M. P., Giovanelli, R. & Marinoni, C., 2007, ApJS, 172, 599S
Tonini, C., Lapi, A., Shankar, F. & Salucci, P., 2006, ApJ, 638L, 13T
Tonini, C., Lapi, A. & Salucci, P., 2006 ApJ, 649, 591T
Tonini, C., Maraston, C., Ziegler, B., Bohm, A., Thomas, D., Devriendt, J. & Silk, J., 2011, MNRAS, 415, 811T
Tonini, C., Bernyk, M., Croton, D., Maraston, C. & Thomas, D., 2012, ApJ, 759, 43T
Tonini, C., 2013, ApJ, 762, 39T
Tully, R.B., & Fisher, J. R., 1977, A&A, 54, 661T
Williams, M. J., Bureau, M. & Cappellari, M., 2010, MNRAS, 409, 1330
Yegorova, I.A. & Salucci, P., 2007, MNRAS, 377, 507Y
Zaritsky, D., Zabludoff, A. I. & Gonzalez, A. H., 2008, ApJ, 682, 68Z